A ribonuclease zymogen activated by the NS3 protease of the hepatitis C virus

R. J. Johnson[1], Shawn R. Lin[1] and Ronald T. Raines[1,2]

1 Department of Biochemistry, University of Wisconsin–Madison, Madison, WI, USA
2 Department of Chemistry, University of Wisconsin–Madison, Madison, WI, USA

Translating proteases as inactive precursors, or zymogens, protects cells from the potentially lethal action of unregulated proteolytic activity. Here, we impose this strategy on bovine pancreatic ribonuclease (RNase A) by creating a zymogen in which quiescent ribonucleolytic activity is activated by the NS3 protease of the hepatitis C virus. Connecting the N-terminus and C-terminus of RNase A with a 14-residue linker was found to diminish its ribonucleolytic activity by both occluding an RNA substrate and dislocating active-site residues, which are devices used by natural zymogens. After cleavage of the linker by the NS3 protease, the ribonucleolytic activity of the RNase A zymogen increased 105-fold. Both before and after activation, the RNase A zymogen displayed high conformational stability and evasion of the endogenous ribonuclease inhibitor protein of the mammalian cytosol. Thus, the creation of ribonuclease zymogens provides a means to control ribonucleolytic activity and has the potential to provide a new class of antiviral chemotherapeutic agents.

Proteolysis is an essential biological activity that requires tight regulation [1,2]. One strategy employed by cells to control proteolysis is to encode proteolytic enzymes as inactive precursors, zymogens [3]. Zymogens are translated with N-terminal polypeptides, or prosegments, that inhibit proteolytic activity, typically by occluding substrate binding [4], distorting the active site [3], or altering the substrate-binding cleft [5,6]. When proteolytic activity is required, the inhibitory N-terminal prosegment is removed by autocatalytic cleavage, by cleavage by another protease, or by a conformational change invoked by the local environment [3].

After processing of a zymogen to a mature protease, a cell can restrict proteolytic activity by employing cellular inhibitors [2,3]. Only this type of regulation is used to control the enzymatic activity of ribonucleases [7,8], which, like proteases, can degrade an essential biopolymer. The regulation of pancreatic-type ribonucleases is accomplished by ribonuclease inhibitor (RI) [9], a cytosolic protein that binds to bovine pancreatic ribonuclease (RNase A, EC 3.1.27.5) [10,11] and its mammalian homologs with extremely high affinity ($K_i \approx 10^{-15}$ M). By evading inhibition by RI, variants of RNase A become toxic to human cells [12–16].

Inspired by protease zymogens, we recently created a zymogen of RNase A in which a 14-residue linker connects the N-terminus and C-terminus [17]. The linker acts like the prosegment of a natural zymogen, inhibiting the native ribonucleolytic activity of RNase A but allowing the manifestation of near-wild-type activity upon cleavage. It contains a sequence recognized by the plasmepsin II protease from the malarial parasite *Plasmodium falciparum*. Incubation with that protease restores the ribonucleolytic activity of RNase A. We reasoned that this strategy could be general, in that the sequence of the linker could correspond to the recognition sequence of other proteases.

Hepatitis C virus (HCV) [18,19], a positive-stranded RNA virus of the family Flaviviridae [20,21], is estimated to infect 170 million people (i.e. 2% of humanity) [22]. This malady can lead to serious liver diseases such as cirrhosis and hepatocellular carcinoma, making infection by HCV the leading indicator of liver transplantation in the United States [23]. Like other RNA viruses, HCV translates its 9.6-kb genome as one single polyprotein, which is then co-translationally and post-translationally cleaved by cellular endopeptidases and viral proteases to form at least four structural and six nonstructural proteins [23]. Nonstructural protein 3 (NS3) of the HCV polyprotein is a chymotrypsin-like serine protease [24]. The NS3 protein is essential for viral replication, cleaving the viral polyprotein at four positions [25,26].

Here, we report on an RNase A zymogen with a linker that corresponds to a sequence cleaved by the HCV NS3 protease. We investigate the physicochemical properties of this RNase A zymogen both before and after its proteolytic activation, including its enzymatic activity, conformational stability, and affinity for RI. Characterization of this zymogen provides new insight into zymogen action. Moreover, the ensuing merger of the attributes of a cytotoxic ribonuclease with an enzymatic activity reliant on the HCV NS3 protease portends a new approach to antiviral therapies.

Results

Zymogen design

As a potential target for antiviral therapy, the HCV NS3 protease has a well-characterized structure and function [27]. The HCV NS3 protease cleaves the HCV viral polyprotein at four specific locations, and the sequences of the cleavage sites are known [25,26]. Of these, the cleavage site between nonstructural proteins 5A and 5B (NS5A/5B) of the HCV polyprotein is cleaved most rapidly [25]. Consequently, the NS5A/5B sequence of EDVV(C/A)CSMSY was chosen as the linker for the HCV RNase A zymogen [25]. For full proteolytic activity, the NS3 protease recognition sequence requires 10 residues of the NS5A/5B sequence with cysteine residues in the P1 and P2 positions, which immediately precede the scissile bond. If the cysteine residue in the P1 position is replaced with alanine, the NS3 protease no longer cleaves the NS5A/5B peptide; a similar mutation at the P2 position results in only a 40% decrease in cleavage activity [25,26]. The proximal cysteines in the NS5A/5B sequence could, however, form a disulfide bond [28]

which would alter the structure of the linker. Therefore, two HCV zymogen constructs were designed, one with a cysteine residue (2C zymogen) in the P2 position and one with an alanine residue there (1C zymogen). These two zymogens contain, in effect, a peptide that links residue 124 (C-terminus) with residue 1 (N-terminus).

In each zymogen, a new N-terminus and C-terminus were created at residues 89 and 88, respectively [17]. Disulfide bonds were used to link residues 88 and 89 and residues 4 and 118, as cystines at these positions had been shown to increase the conformational stability of other RNase A variants by 10 and 5 °C, respectively [17,29]. A model of the 2C zymogen is shown in Fig. 1, highlighting the location of all seven possible disulfide bonds and the new termini at positions 89 and 88.

Activation of ribonucleolytic activity

An essential aspect of a functional zymogen is the resistance of the parent enzyme to cleavage by the activating protease. Accordingly, wild-type RNase A (25 μM) was incubated for 60 min at 37 °C with equimolar NS4A/NS3 protease. After incubation, wild-type RNase A exhibited no significant loss in ribonucleolytic activity. Thus, RNase A is not a substrate for the NS4A/NS3 protease.
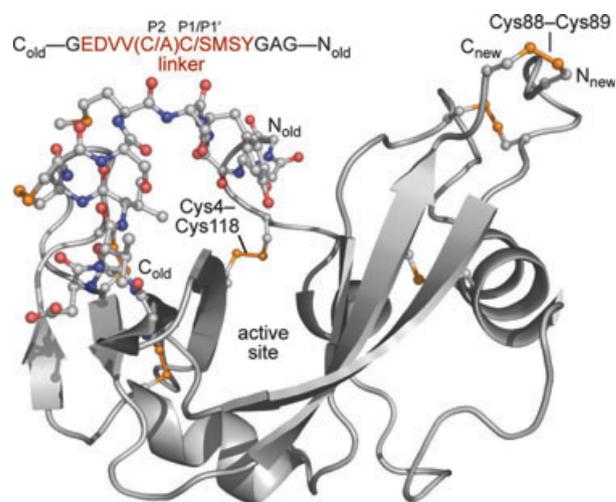

Fig. 1. Structural model of unactivated 2C zymogen with 88/89 termini, 14-residue linker, and seven disulfide bonds. The conformational energy of the side chains of the variant residues were minimized with the program SYBYL (Tripos). Atoms of the linker and cysteine residues are shown explicitly; non-native cystines and old and new termini are labeled. The sequence of the linker is given with flexible residues in black, the NS5A/5B cleavage sequence in red, and the scissile bond designated with a solidus ('/').
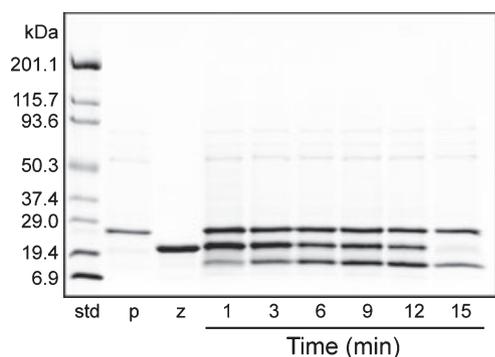
Fig. 2. Activation of 1C zymogen by the NS4A/NS3 protease. Activation at 37 °C was monitored at different times after the addition of 0.5 molar equivalents of NS4A/NS3 protease by SDS/PAGE in the presence of dithiothreitol. std, Protein molecular mass standard; p, NS4A/NS3 protease after a 15-min incubation at 37 °C; z, 1C zymogen after a 15-min incubation at 37 °C.
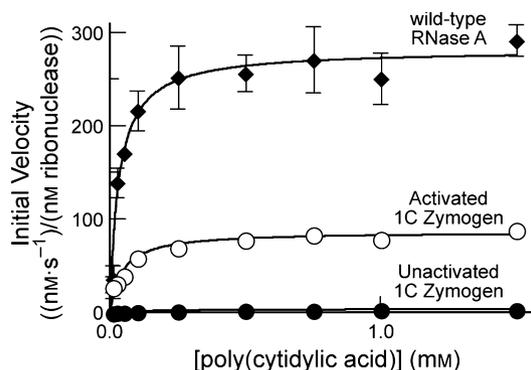

Fig. 3. Ribonucleolytic activity of unactivated 1C zymogen (●, 1.0 μM), activated 1C zymogen (○, 6 nM), and wild-type RNase A (◆, 1.5 nM). Initial velocity data (v/[ribonuclease]) were determined at increasing concentrations of poly(C). Data points are the mean of three independent assays, and are shown ± SE. Data were used to determine the values of k_{cat}, K_m, and k_{cat}/K_m (Table 1).

An RNase A zymogen should, however, be a substrate for its cognate protease but not other common proteases. The expected mass of the fragments produced by cleavage of the 1C zymogen and reduction of its disulfide bonds are 10.5 kDa (which is readily detectable by SDS/PAGE) and 4.6 kDa. Incubation of the 1C zymogen with a substoichiometric quantity of NS4A/NS3 protease led to its nearly complete processing after 15 min at 37 °C, as shown in Fig. 2. Incubation of the 1C zymogen for 15 min at 37 °C with trypsin, which is a common protease with high enzymatic activity, resulted in insignificant cleavage (molar ratio 1 : 100 or 1 : 25 trypsin/1C zymogen; data not shown).

An RNase A zymogen should also have low ribonucleolytic activity before activation, and should regain nearly wild-type activity upon incubation with the NS4A/NS3 protease. The initial rates of poly(C) cleavage by unactivated 1C zymogen, activated 1C zymogen, and RNase A are depicted in Fig. 3, and the resulting steady-state kinetic parameters are listed in Table 1. The k_{cat}/K_m value for the cleavage of poly(C) by wild-type RNase A is higher than that reported previously [30] because of the removal from the assay

buffer of oligomeric vinylsulfonic acid, which is a potent inhibitor of RNase A [31].

Wild-type RNase A has 430-fold and 10^4-fold higher k_{cat}/K_m values for poly(C) cleavage than the unactivated 1C and 2C zymogens, respectively (Table 1). The decreased activity of unactivated zymogens is a result of both a smaller value of k_{cat} and a larger value of K_m. The k_{cat}/K_m value of the unactivated 1C zymogen is 33-fold higher than that of the unactivated 2C zymogen, and the difference is again the result of both a decrease in k_{cat} and an increase in K_m. The increase in k_{cat} on activation of the 1C and 2C zymogens suggests that the intact linker dislocates key catalytic residues.

The only difference between the unactivated 2C and 1C zymogens is the sulfur atom of the cysteine residue in the P2 position of the 2C zymogen. This difference enables the two adjacent cysteine residues in the linker of 2C zymogen to form a disulfide bond. A reaction with 5,5′-dithiobis(2-nitrobenzoic acid) (Nbs$_2$) was used to determine the number of free thiols in the 1C and 2C zymogens. The results indicate that the 1C and 2C zymogens have 0.6 ± 0.1 and 0.16 ± 0.04 free thiols per molecule, respectively [32]. These values suggest that the cysteine residues in the linker of the 2C

Table 1. Enzymatic activity of ribonuclease A zymogens. Values of k_{cat}, K_m, and k_{cat}/K_m (± SE) were determined for catalysis of poly(C) cleavage at 25 °C in 0.10 M Mes/NaOH buffer (oligomeric vinylsulfonic acid-free), pH 6.0, containing NaCl (0.10 M). Initial velocity data were used to calculate values of k_{cat}, K_m, and k_{cat}/K_m with the program DELTAGRAPH 5.5.

Ribonuclease	$(k_{cat})_{unactivated}$ (s^{-1})	$(k_{cat})_{activated}$ (s^{-1})	$(K_m)_{unactivated}$ (10^{-6} M)	$(K_m)_{activated}$ (10^{-6} M)	$(k_{cat}/K_m)_{unactivated}$ (10^3 M^{-1}·s^{-1})	$(k_{cat}/K_m)_{activated}$ (10^3 M^{-1}·s^{-1})	$(k_{cat}/K_m)_{activated}/$ $(k_{cat}/K_m)_{unactivated}$
Wild-type	—	280 ± 29	—	33 ± 2	—	8300 ± 700	—
1C zymogen	3.8 ± 0.1	86 ± 5	200 ± 20	43 ± 7	19 ± 2	2000 ± 300	105
2C zymogen	0.70 ± 0.02	10 ± 1	1200 ± 10	1400 ± 200	0.58 ± 0.04	7.4 ± 0.4	13

zymogen do indeed form a disulfide bond. Disulfide bonds between adjacent cysteine residues can distort the conformation of an enzyme and diminish its catalytic activity [33]. This effect is probably responsible for the ribonucleolytic activity of the unactivated 2C zymogen being lower than that of the unactivated 1C zymogen (Table 1). These data also suggest that the cysteine residue in the linker of 1C zymogen is at least partially buried in the unactivated zymogen, as the 1C zymogen appears to have 0.6 instead of 1.0 free cysteines.

On incubation with the NS4A/NS3 protease, the K_m of activated 1C zymogen returns to wild-type values, and the k_{cat} is one-third times that of the wild-type enzyme, giving a k_{cat}/K_m value that is one-quarter that of wild-type RNase A (Table 1). The change in both kinetic parameters on activation suggests that the linker affects substrate binding and turnover by an unactivated RNase A zymogen, but that these effects are reversible. The disulfide bond in the linker of activated 2C zymogen also influences the catalytic activity, as both its k_{cat} and K_m values remain lower than those of activated 1C zymogen.

The ratio of the $(k_{cat}/K_m)_{activated}$ value to the $(k_{cat}/K_m)_{unactivated}$ value provides an estimate of the effectiveness of the linker in modulating the ribonucleolytic activity and, in essence, provides a measure of the therapeutic index of a ribonuclease zymogen. For the 1C zymogen, the $(k_{cat}/K_m)_{activated}/(k_{cat}/K_m)_{unactivated}$ ratio is 105 for the 1C zymogen and 13 for the 2C zymogen. Overall, the disulfide bond formed between the cysteine residues in the linker of the 2C zymogen seems to be detrimental to the ability of the linker to act as a zymogen prosegment. Accordingly, only the 1C zymogen was subjected to additional biochemical analyses.

Zymogen conformation and conformational stability

The near-UV CD spectrum (170–250 nm) of a protein is a representation of protein secondary structure [34]. The CD spectra of unactivated and activated 1C zymogen are shown in Fig. 4A. Although deconvolution of the contribution of distinct secondary-structure elements to the CD spectra of unactivated and activated 1C zymogen is difficult, activation of the 1C zymogen appears to have an effect on its CD spectrum and is thus likely to affect its conformation.

The conformational stability of both unactivated and activated 1C zymogen was determined by CD spectroscopy. The thermal denaturation curves are shown in Fig. 4B, and the resulting values of T_m are listed in Table 2. Both unactivated and activated 1C
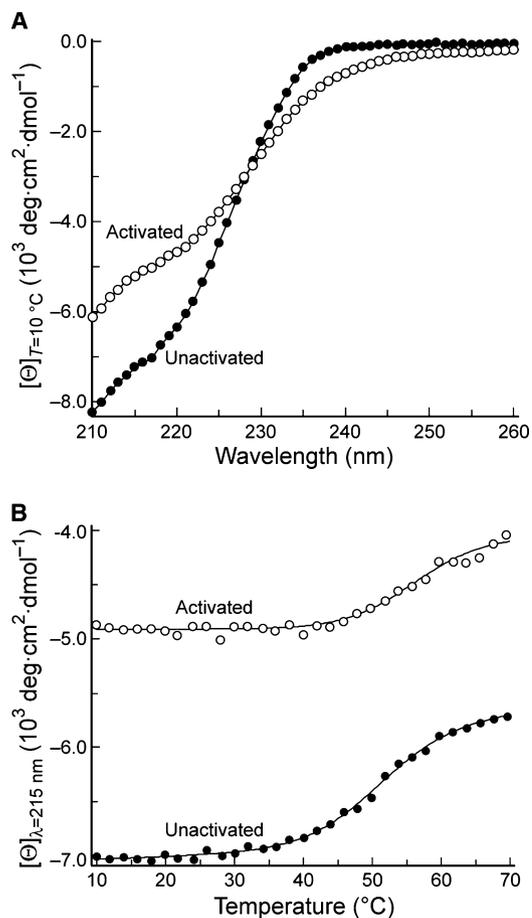

Fig. 4. Conformation and conformational stability of unactivated (●) and activated (○) 1C zymogens assessed by CD. (A) Near-UV CD spectra of unactivated and activated 1C zymogens (0.5 mg·mL^{-1} in NaCl/P$_i$). (B) Thermal denaturation of unactivated and activated 1C zymogens (0.5 mg·mL^{-1} in NaCl/P$_i$). Molar ellipticity at 215 nm was monitored after a 2-min equilibration at each temperature. Data were fitted to a two-state model to determine values of T_m (Table 2).

zymogen have T_m values well above physiological temperature (37 °C) but below that of wild-type RNase A (64 °C). As with the RNase A zymogen described previously [17], the conformational stability of the 1C zymogen increases on activation, perhaps as the result of the release of strain.

Affinity for ribonuclease inhibitor and cytotoxicity

RI recognizes members of the RNase A superfamily with femtomolar affinity [8]. As many RI contacts with RNase A are in the active site [35], the linker in an RNase A zymogen could block RI binding. The affinity of porcine ribonuclease inhibitor (pRI) for the 1C zymogen was determined by using a competitive binding assay with fluorescein-labeled G88R RNase A [36]. The resulting K_d values for the complexes of pRI

Table 2. Physicochemical properties of a ribonuclease A zymogen.

Ribonuclease	$(T_m)_{unactivated}$[a] (°C)	$(T_m)_{activated}$[a] (°C)	$(K_d)_{unactivated}$[b] (nM)	$(K_d)_{activated}$[b] (nM)	$(IC_{50})_{unactivated}$[c] (μM)
Wild-type	64[d]	—	44×10^{-6e}	—	> 25
1C zymogen	51.6 ± 0.4	56.3 ± 0.7	> (10^3)	13 ± 0.2	> 25

[a] Values of T_m for HCV zymogens were determined in NaCl/P$_i$ by CD spectroscopy. [b] Values of K_d (± SE) were determined for the complex with pRI at 23 (± 2) °C. [c] Values of IC$_{50}$ are for the incorporation of [methyl-^{3}H]thymidine into the DNA of K-562 cells treated with a ribonuclease, and were calculated with Eqn (1). [d] From Rutkoski *et al.* [37]. [e] From Vicentini *et al.* [52] for the pRI–RNase A complex.

with both unactivated and activated 1C zymogen are listed in Table 2. Unactivated 1C zymogen at 16 μM did not compete with fluorescein-labeled G88R RNase A for binding to pRI, and the K_d value for the pRI complex with unactivated 1C zymogen was therefore estimated to be > 1 μM [37]. The lack of affinity of unactivated 1C zymogen for pRI puts it in the range of the most RI-evasive of known RNase A variants [37]. Yet, unlike most RI-evasive variants, unactivated 1C zymogen was not toxic (IC$_{50}$ > 25 μM) to a standard cancer cell line used to estimate ribonuclease cytotoxicity (Table 2).

In contrast, the value of K_d (= 13 nM) for the complex of pRI with activated 1C zymogen is greater than that of the unactivated 1C zymogen. Yet, the affinity of pRI for wild-type RNase A is still 10^5-fold higher than that for the activated 1C zymogen (Table 2), suggesting that the cleaved linker still disturbs RI binding. The affinity of pRI for activated 1C zymogen is close to that measured previously for K7A/G88R RNase A ($K_d = 17$ nM) [37]. The change in binding affinity of pRI for unactivated and activated 1C zymogen provides additional evidence that the linker is flexible and that it moves away from the RNase A active site on activation.

Discussion

Basis for zymogen inactivity

The cleavage of a peptide bond in natural zymogens leads to their activation by enabling the binding of substrate [38], altering the conformation of active-site residues [3], or constituting the substrate binding cleft [5,6]. For example, formation of the 'oxyanion hole' and substrate binding cleft occurs on activation of chymotrypsinogen [3,5]. Based on our molecular modeling, the linker of the RNase A zymogen appears to occlude the binding of substrate to the active site (Fig. 1). This model is supported by the low K_m values of the unactivated 1C and 2C zymogens (Table 1). Likewise, the intact linker of the unactivated zymogen inhibits RI binding to the active site more than the

cleaved linker (Table 2). Still, the cleaved linker, which is not excised from the zymogen, continues to instill the ability to evade RI upon the activated zymogen. This continued evasion contrasts with the behavior of some natural zymogens, which bind tightly to endogenous inhibitors upon activation [2,3].

If the linker merely occludes the substrate from binding to the RNase A zymogens and has no influence on the conformation of active-site residues, then activation would have no effect on the turnover number (k_{cat}) [38]. Yet, the k_{cat} values for the unactivated 1C zymogen (3.8 s^{-1}) and 2C zymogen (0.70 s^{-1}) are significantly lower than those of the activated zymogens (Table 1). This decrease in k_{cat} before activation suggests that key active-site residues are dislocated by the intact linker. Changes in the CD spectra on activation are likewise indicative of a conformational change (Fig. 4).

Consequently, the low activity of the RNase A zymogen appears to arise from both substrate occlusion and an alteration in active-site residues. Thus, two strategies used by natural zymogens [3,38] are replicated in our artificial one. Most importantly, the intact linker diminishes the ribonucleolytic activity of the 1C zymogen, but allows its reconstitution upon cleavage.

Therapeutic potential

The NS3 protease of HCV is a major drug target [39]. Design of small-molecule inhibitors of the NS3 protease is, however, problematic because of its shallow substrate-binding cleft [40–42]. Herein, we take the opposite tack. Rather than trying to inhibit the enzymatic activity of the NS3 protease, we attempt to exploit this activity to activate an RNase A zymogen.

By comparing the ribonucleolytic activity and RI affinity of unactivated and activated 1C zymogen with those of other RNase A variants, we can estimate the therapeutic potential of an HCV RNase A zymogen. Unactivated 1C zymogen was not toxic to K-562 cells (Table 2) and has ribonucleolytic activity comparable to those of nontoxic ribonucleases, such as K41A/G88R RNase A [43,44]. Upon activation, the

ribonucleolytic activity of the 1C RNase A zymogen increases 105-fold, approaching that of wild-type RNase A. Combining the ribonucleolytic activity of the activated 1C zymogen with its affinity for RI enables an estimate of its toxicity to cells containing the NS3 protease [37,44]. For example, the activated 1C zymogen has greater ribonucleolytic activity than K7A/G88R RNase A and similar RI affinity [37]. K7A/G88R RNase A has $IC_{50} = 1.1$ μM for K-562 cell proliferation.

In conjunction with a positive activation ratio, the 1C zymogen also combines an increased T_m upon activation, making the activated ribonuclease more stable than the unactivated one. Thus, 1C RNase A zymogen has the necessary attributes for selective cytotoxicity to HCV, including a high $(k_{cat}/K_m)_{activated}/(k_{cat}/K_m)_{unactivated}$ ratio (105-fold), high conformational stability, and an ability to evade RI. Testing the toxicity of an RI-evasive 1C zymogen for HCV-infected cells (as opposed to K-562 cells; Table 2) is thus a worthwhile goal.

Conclusions

Unchecked ribonucleolytic activity is potentially lethal to cells, which have evolved RI to modulate this activity [7,45]. Transforming ribonucleases into zymogens represents another general strategy for controlling ribonucleolytic activity. We have developed an RNase A zymogen that is activated by the NS3 protease of HCV. The linker of our RNase A zymogen inhibits its activity by a mechanism similar to proteolytic zymogens, by sterically blocking substrate binding to the ribonuclease active site and dislocating key active-site residues. The linker of RNase A zymogens could have an additional role in ribonuclease cytotoxicity by decreasing the affinity of RI for RNase A, even after activation. The HCV RNase A zymogen has the necessary characteristics of a ribonuclease therapeutic, including wild-type activity after activation, a T_m value above physiological temperature, and low affinity for RI. By exploiting the proteolytic activity of NS3, RNase A zymogens could be selectively activated to circumvent the known mechanisms of microbial resistance, allowing development of a ribonuclease-based treatment for HCV.

Experimental procedures

Materials

Escherichia coli BL21(DE3) and pET28a(+) were from Novagen (Madison, WI, USA). Enzymes were obtained from Promega (Madison, WI, USA). Protein purification columns were from Amersham Biosciences (Piscataway, NJ, USA). Mes buffer (Sigma–Aldrich, St Louis, MO, USA) was purified by anion-exchange chromatography to remove trace amounts of oligomeric vinylsulfonic acid [31]. Poly(C) (Sigma–Aldrich) was precipitated with ethanol before its use to remove short RNA fragments. All other chemicals were of commercial grade or better and used without further purification.

NaCl/P_i contained (in 1 litre) NaCl (8.0 g), KCl (2.0 g), Na$_2$HPO$_4$·7H$_2$0 (1.15 g), KH$_2$PO$_4$ (2.0 g), and NaN$_3$ (0.10 g) and had a pH of 7.4.

Instrumentation

CD experiments were performed with a model 62A DS CD spectrometer (Aviv, Lakewood, NJ, USA) equipped with a temperature controller. The mass of RNase A zymogens was confirmed by MALDI-TOF MS using a Voyager-DE-PRO Biospectrometry Workstation (Applied Biosystems, Foster City, CA, USA). CD and MALDI–TOF MS experiments were performed at the Biophysics Instrumentation Facility, University of Wisconsin–Madison, Madison, WI, USA.

UV–visible spectroscopy was performed with a Cary 3 double-beam spectrophotometer equipped with a Cary temperature controller (Varian, Palo Alto, CA, USA). Fluorescence spectroscopy was performed with a QuantaMaster 1 photon-counting fluorimeter equipped with sample stirring (Photon Technology International, South Brunswick, NJ, USA).

Zymogen preparation

Plasmids that direct the production of HCV RNase A zymogens were derived from plasmid pET22b(+)/19N [17]. The linker-encoding region of that plasmid was replaced with DNA encoding GEDVVCCSMSYGAG (to yield the '2C' zymogen) or GEDVVACSMSYGAG (to yield the '1C' zymogen) by using the QuikChange mutagenesis kit (Stratagene, La Jolla, CA, USA). These sequences correspond to preferred NS5A/5B recognition sequences of the NS3 protease [25,26]. The production, folding, and purification of RNase A zymogens were performed as described for other RNase A variants [30], except that oxidative folding was performed for a minimum of 72 h at 4 °C and pH 7.8 with 0.5 M arginine in the folding buffer (1C *m/z* 15 142, expected 15 116; 2C *m/z* 15 162, expected 15 148).

Protease preparation

Clone B cells [46] were a gift from C. M. Rice (The Rockefeller University, New York, NY, USA). Total cellular RNA was isolated from these cells by using the TRIZOL

reagent (Invitrogen, Carlsbad, CA, USA) [46,47]. A one-step RT-PCR kit (Qiagen, Valencia, CA, USA) was used to amplify DNA encoding residues 1–181 of the NS3 gene, flanked by *Nde*I and *Xho*I restriction sites [48]. The resulting DNA fragment was inserted into plasmid pET-28a(+), which encodes an N-terminal His$_6$ tag. As in previous systems to produce the NS3 protease [48], DNA encoding 12 residues of the NS4A protein of HCV and a flexible Gly-Ser-Gly-Ser tether was inserted upstream of the NS3 gene. The protein encoded by the resulting plasmid is referred to as the 'NS4A/NS3 protease'.

NS4A/NS3 protease was purified by methods published previously [48] and found to be > 95% pure by SDS/PAGE and had the expected molecular mass (*m/z* 21 424, expected 21 407). Purified NS4A/NS3 protease was dialyzed exhaustively against 50 mM Tris/HCl buffer, pH 7.5, containing NaCl (0.30 M), glycerol (10%, v/v), Tween 20 (0.025%, v/v), and dithiothreitol (0.005 M), and aliquots were flash-frozen at −80 °C. The enzymatic activity of purified NS4A/NS3 was assayed by monitoring the change in retention time of a fluorescent peptide substrate (Bachem, King of Prussia, PA, USA) during reverse-phase C$_{18}$ HPLC. An inactive variant of NS4A/NS3 protease with Ser139 replaced with an alanine residue did not cleave the fluorescent substrate, as had been reported previously [24].

Detection of thiol groups

Nbs$_2$ reacts with thiol groups (but not disulfide bonds) to produce a yellow chromophore that can be used to quantitate the number of thiol groups [32]. Solutions of the 1C and 2C zymogens were diluted to concentrations of 0.00625, 0.01325, 0.0265, and 0.053 mM with 100 mM Tris/HCl buffer, pH 8.3, containing EDTA (0.01 M). A 10-fold molar excess of Nbs$_2$ [as 50 mM Tris/HCl buffer, pH 7.5, containing NaCl (0.10 M), EDTA (0.05 M), and Nbs$_2$ (0.005 M)] was added to each dilution, and the Nbs$_2$ was allowed to react for 30 min at 25 °C. The number of free cysteines was determined by UV absorption using $\varepsilon_{412\ nm} = 14.15$ M^{-1}·cm^{-1} for 2-nitro-5-thiobenzoic acid [32].

Activation of zymogens

RNase A zymogens were activated by mixing them with 0.5 molar equivalents of NS4A/NS3 protease in reaction buffer {50 mM Tris/HCl buffer, pH 7.5, containing NaCl (0.3 M), glycerol (10%, v/v), Tween 20 (0.025%, v/v), and dithiothreitol (0.005 M) [48]}, and incubating the resulting mixture at 37 °C for 15 min. Activation was stopped by dilution (1 : > 10) into 0.10 M Mes/NaOH buffer, pH 6.0, containing NaCl (0.10 M) and placement of the reaction mixture on ice. Reaction mixtures were subjected to SDS/PAGE in the presence of dithiothreitol to assess zymogen activation.

Ribonucleolytic activity

The ability of a ribonuclease to catalyze the cleavage of poly(C) ($\varepsilon_{268\ nm} = 6200$ M^{-1}·cm^{-1} per nucleotide) was monitored by measuring the increase in UV absorption upon cleavage ($\Delta\varepsilon_{250\ nm} = 2380$ M^{-1}·cm^{-1} [30]). Assays were performed at 25 °C in 0.10 M Mes/NaOH buffer, pH 6.0, containing NaCl (0.10 M), poly(C) (10 μM to 1.5 mM), and enzyme (1.5 nM for wild-type RNase A; 1 and 3 μM for the 1C and 2C unactivated zymogens, respectively; 6 and 100 nM for the 1C and 2C activated zymogens, respectively). Initial velocity data were used to calculate values of k_{cat}, K_m, and k_{cat}/K_m with the program DELTAGRAPH 5.5 (Red Rock Software, Salt Lake City, UT, USA).

Zymogen conformation and conformational stability

CD spectroscopy was used to assess the conformation of the unactivated and activated 1C zymogens. A solution of zymogen (0.5 mg·mL^{-1} in NaCl/P$_i$) was incubated for 5 min at 10 °C, and a CD spectrum was acquired from 260 to 210 nm in 1-nm increments.

CD spectroscopy was also used to evaluate the conformational stability of the unactivated and activated 1C zymogens [49]. A solution of zymogen (0.5 mg·mL^{-1} in NaCl/P$_i$) was heated from 10 to 80 °C in 2 °C increments, and the change in molar ellipticity at 215 nm was monitored after a 2-min equilibration at each temperature. RNase A zymogens were activated as before, and NS4A/NS3 protease was removed from the reaction mixture by using His-Select spin columns (Sigma–Aldrich). CD spectra were fitted to a two-state model for denaturation to determine the value of T_m.

Ribonuclease inhibitor evasion

pRI was purified as described previously [50]. The affinity of the unactivated and activated 1C zymogen for pRI was determined using a fluorescent competition assay described previously, with minor modifications [36]. Briefly, fluorescein-labeled G88R RNase A (50 nM) and various concentrations of unlabeled RNase A zymogen were added to 2.0 mL NaCl/P$_i$ containing dithiothreitol (5 mM), and the resulting solution was incubated at 23 (± 2) °C for 20 min. After this incubation, the initial fluorescence intensity of the unbound fluorescein-labeled G88R RNase A was monitored for 3 min (excitation 491 nm; emission 511 nm). pRI was then added to 50 nM, and the final fluorescence intensity was measured. K_d values were obtained by nonlinear least-squares analysis of the binding isotherm with the program DELTAGRAPH 5.5. The K_d value for the complex between pRI and fluorescein-labeled G88R RNase A was assumed to be 0.52 nM [36].

Cytotoxic activity

The effect of an RNase A zymogen on the proliferation of K-562 cells was assayed as described previously [17,37]. After a 44-h incubation with a ribonuclease, K-562 cells were treated with [methyl-^{3}H]thymidine for 4 h, and the incorporation of radioactive thymidine into the cellular DNA was quantified by liquid-scintillation counting. Results were the percentage of [methyl-^{3}H]thymidine incorporated into the DNA compared with the incorporation into control K-562 cells to which only NaCl/P_i was added. Data were the mean of three measurements for each concentration, and the entire experiment was performed in duplicate. IC_{50} values were calculated by fitting the curves by nonlinear regression to a sigmoidal dose–response curve with the equation:

$$y = \frac{100\%}{1 + 10^{(\log(IC_{50}) - \log[\text{ribonuclease}])h}} \tag{1}$$

where y is total DNA synthesis after the [methyl-^{3}H]thymidine pulse, and h is the slope of the curve.

Molecular modeling

The atomic co-ordinates of RNase A were obtained from the Protein Data Bank (accession code 7RSA) [51]. Models of both 1C and 2C RNase A zymogen were created with the program SYBYL (Tripos, St Louis, MO, USA) on an O2 computer (Silicon Graphics, Mountain View, CA, USA) [17]. SYBYL was used to connect the old N-termini and C-termini via the 14-residue linker, to replace residues 4, 88, 89, and 118 with cysteine, to cleave the polypeptide chain between residues 88 and 89, to create disulfide bonds between residues 4 and 118 and residues 88 and 89, and to minimize the conformational energy of the new residues [17].

Acknowledgements

We are grateful to Dr C. M. Rice for the gift of the Clone B cell line, and to R. F. Turcotte, L. D. Lavis, and Dr M. T. Borra for contributive discussions.

References

1 Neurath H (1984) Evolution of proteolytic enzymes. *Science* **224**, 350–357.

2 Salvesen GS & Abrams JM (2004) Caspase activation: stepping on the gas or releasing the brakes? Lessons from humans and flies. *Oncogene* **23**, 2774–2784.

3 Khan AR & James MN (1998) Molecular mechanisms for the conversion of zymogens to active proteolytic enzymes. *Protein Sci* **7**, 815–836.

4 Borgono CA & Diamandis EP (2004) The emerging roles of human tissue kallikreins in cancer. *Nat Rev Cancer* **4**, 876–890.

5 Freer ST, Kraut J, Robertus JD, Wright HT & Xuong NH (1970) Chymotrypsinogen: 2.5-Å crystal structure, comparison with α-chymotrypsin, and implications for zymogen activation. *Biochemistry* **9**, 1997–2009.

6 Kossiakoff AA, Chambers JL, Kay LM & Stroud RM (1977) Structure of bovine trypsinogen at 1.9 Å resolution. *Biochemistry* **16**, 654–664.

7 Haigis MC, Kurten EL & Raines RT (2003) Ribonuclease inhibitor as an intracellular sentry. *Nucleic Acids Res* **31**, 1024–1032.

8 Dickson KA, Haigis MC & Raines RT (2005) Ribonuclease inhibitor: structure and function. *Prog Nucleic Acid Res Mol Biol* **80**, 349–374.

9 Lee FS, Shapiro R & Vallee BL (1989) Tight-binding inhibition of angiogenin and ribonuclease A by placental ribonuclease inhibitor. *Biochemistry* **28**, 225–230.

10 Cuchillo CM, Vilanova M & Nogués MV (1997) Pancreatic ribonucleases. In *Ribonucleases: Structures and Functions* (D'Alessio G & Riordan JF, eds), pp. 271–304. Academic Press, New York, NY.

11 Raines RT (1998) Ribonuclease A. *Chem Rev* **98**, 1045–1065.

12 Matoušek J (2001) Ribonucleases and their antitumor activity. *Comp Biochem Physiol* **129C**, 175–191.

13 Leland PA & Raines RT (2001) Cancer chemotherapy: ribonucleases to the rescue. *Chem Biol* **8**, 405–413.

14 Makarov AA & Ilinskaya ON (2003) Cytotoxic ribonucleases: molecular weapons and their targets. *FEBS Lett* **540**, 15–20.

15 Loverix S & Steyaert J (2003) Ribonucleases and their anti-tumor activity. *Comp Biochem Physiol* **129C**, 175–191.

16 Arnold U & Ulbrich-Hofmann R (2006) Natural and engineered ribonucleases as potential cancer therapeutics. *Biotechnol Lett* **28**, 1615–1622.

17 Plainkum P, Fuchs SM, Wiyakrutta S & Raines RT (2003) Creation of a zymogen. *Nat Struct Biol* **10**, 115–119.

18 Major ME, Rehermann B & Feinstone SM (2001) Hepatitis C viruses. In *Fields Virology* (Knipe, DM & Howley, PM, eds), 4th edn, pp. 1127–1161. Lippincott, Williams & Wilkins, New York, NY.

19 Lindenbach BD & Rice CM (2005) Unravelling hepatitis C virus replication from genome to function. *Nature* **436**, 933–938.

20 Lindenbach BD & Rice CM (2001) *Flaviviridae*: the viruses and their replication. In *Fields Virology* (Knipe, DM & Howley, PM, eds), 4th edn, pp. 991–1041. Lippincott, Williams & Wilkins, New York, NY.

21 Burke DS & Monath TP (2001) Flaviviruses. In *Fields Virology* (Knipe, DM & Howley, PM, eds), pp. 1043–1125. Lippincott, Williams & Wilkins, New York, NY.

22 World Health Organization (1999) Global surveillance and control of hepatitis C. Report of a WHO Consultation organized in collaboration with the Viral

Hepatitis Prevention Board, Antwerp, Belgium. *J Viral Hepat* **6**, 35–47.

23 Fishman JA, Rubin RH, Koziel MJ & Periera BJ (1996) Hepatitis C virus and organ transplantation. *Transplantation* **62**, 147–154.

24 Tomei L, Failla C, Santolini E, De Francesco R & La Monica N (1993) NS3 is a serine protease required for processing of hepatitis C virus polyprotein. *J Virol* **67**, 4017–4026.

25 Zhang R, Durkin J, Windsor WT, McNemar C, Ramanathan L & Le HV (1997) Probing the substrate specificity of hepatitis C virus NS3 serine protease by using synthetic peptides. *J Virol* **71**, 6208–6213.

26 Urbani A, Bianchi E, Narjes F, Tramontano A, De Francesco R, Steinkuhler C & Pessi A (1997) Substrate specificity of the hepatitis C virus serine protease NS3. *J Biol Chem* **272**, 9204–9209.

27 Gordon CP & Keller PA (2006) Control of hepatitis C: a medical chemistry perspective. *J Med Chem* **48**, 1–20.

28 Zhang R & Snyder GH (1989) Dependence of formation of small disulfide loops in two-cysteine peptides on the number and types of intervening amino acids. *J Biol Chem* **264**, 18472–18479.

29 Klink TA & Raines RT (2000) Conformational stability is a determinant of ribonuclease A cytotoxicity. *J Biol Chem* **275**, 17463–17467.

30 Leland PA, Schultz LW, Kim B-M & Raines RT (1998) Ribonuclease A variants with potent cytotoxic activity. *Proc Natl Acad Sci USA* **98**, 10407–10412.

31 Smith BD, Soellner MB & Raines RT (2003) Potent inhibition of ribonuclease A by oligo (vinylsulfonic acid). *J Biol Chem* **278**, 20934–20938.

32 Riddles PW, Blakeley RL & Zerner B (1983) Reassessment of Ellman's reagent. *Methods Enzymol* **91**, 49–60.

33 Park C & Raines RT (2001) Adjacent cysteine residues as a redox switch. *Protein Eng* **14**, 939–942.

34 Kelly SM, Jess TJ & Price NC (2005) How to study proteins by circular dichroism. *Biochim Biophys Acta* **1751**, 119–139.

35 Kobe B & Deisenhofer J (1995) A structural basis of the interactions between leucine-rich repeats and protein ligands. *Nature* **374**, 183–186.

36 Abel RL, Haigis MC, Park C & Raines RT (2002) Fluorescence assay for the binding of ribonuclease A to the ribonuclease inhibitor protein. *Anal Biochem* **306**, 100–107.

37 Rutkoski TJ, Kurten EL, Mitchell JC & Raines RT (2005) Disruption of shape-complementarity markers to create cytotoxic variants of ribonuclease A. *J Mol Biol* **354**, 41–54.

38 Sohl JL, Shiau AK, Rader SD, Wilk BJ & Agard DA (1997) Inhibition of α-lytic protease by pro region C-terminal steric occlusion of the active site. *Biochemistry* **36**, 3894–3902.

39 Tan SL, Pause A, Shi Y & Sonenberg N (2002) Hepatitis C therapeutics: current status and emerging strategies. *Nat Rev Drug Discov* **1**, 867–881.

40 Pizzi E, Tramontano A, Tomei L, La Monica N, Failla C, Sardana M, Wood T & De Francesco R (1994) Molecular model of the specificity pocket of the hepatitis C virus protease: implications for substrate recognition. *Proc Natl Acad Sci USA* **91**, 888–892.

41 Kim JL, Morgenstern KA, Lin C, Fox T, Dwyer MD, Landro JA, Chambers SP, Markland W, Lepre CA, O'Malley ET, *et al.* (1996) Crystal structure of the hepatitis C virus NS3 protease domain complexed with a synthetic NS4A cofactor peptide. *Cell* **87**, 343–355.

42 Yao N, Reichert P, Taremi SS, Prosise WW & Weber PC (1999) Molecular views of viral polyprotein processing revealed by the crystal structure of the hepatitis C virus bifunctional protease-helicase. *Struct Fold Des* **7**, 1353–1363.

43 Thompson JE, Kutateladze TG, Schuster MC, Venegas FD, Messmore JM & Raines RT (1995) Limits to catalysis by ribonuclease A. *Bioorg Chem* **23**, 471–481.

44 Bretscher LE, Abel RL & Raines RT (2000) A ribonuclease A variant with low catalytic activity but high cytotoxicity. *J Biol Chem* **275**, 9893–9896.

45 Haigis MC, Haag ES & Raines RT (2002) Evolution of ribonuclease inhibitor protein by exon duplication. *Mol Biol Evol* **19**, 960–964.

46 Blight KJ, Kolykhalov AA & Rice CM (2000) Efficient initiation of HCV RNA replication in cell culture. *Science* **290**, 1972–1974.

47 Lohmann V, Korner F, Koch J, Herian U, Theilmann L & Bartenschlager R (1999) Replication of subgenomic hepatitis C virus RNAs in a hepatoma cell line. *Science* **285**, 110–113.

48 Taremi SS, Beyer B, Maher M, Yao N, Prosise W, Weber PC & Malcolm BA (1998) Construction, expression, and characterization of a novel fully activated recombinant single-chain hepatitis C virus protease. *Protein Sci* **7**, 2143–2149.

49 Lee JE & Raines RT (2003) Contribution of active-site residues to the function of onconase, a ribonuclease with antitumoral activity. *Biochemistry* **42**, 11443–11450.

50 Klink TA, Vicentini AM, Hofsteenge J & Raines RT (2001) High-level soluble production and characterization of porcine ribonuclease inhibitor. *Protein Expr Purif* **22**, 174–179.

51 Wlodawer A, Svensson LA, Sjölin L & Gilliland GL (1988) Structure of phosphate-free ribonuclease A refined at 1.26 Å. *Biochemistry* **27**, 2705–2717.

52 Vicentini AM, Kieffer B, Mathies R, Meyhack B, Hemmings BA, Stone SR & Hofsteenge J (1990) Protein chemical and kinetic characterization of recombinant porcine ribonuclease inhibitor expressed in *Saccharomyces cerevisiae*. *Biochemistry* **29**, 8827–8834.